Chemical Science

ROYAL SOCIETY OF CHEMISTRY

EDGE ARTICLE

View Article Online
View Journal | View Issue

Cite this: *Chem. Sci.*, 2020, **11**, 4773

All publication charges for this article have been paid for by the Royal Society of Chemistry

A fluorescent molecular imaging probe with selectivity for soluble tau aggregated protein†

Yanyan Zhao, ‡[a] Ole Tietz, ‡[a] Wei-Li Kuan,[b] Abdul K. Haji-Dheere,[a] Stephen Thompson,[a] Benjamin Vallin,[b] Elisabetta Ronchi,[a] Gergely Tóth,[c] David Klenerman[de] and Franklin I. Aigbirhio *[a]

Received 6th November 2019
Accepted 19th April 2020

DOI: 10.1039/c9sc05620c

rsc.li/chemical-science

Soluble forms of aggregated tau misfolded protein, generally termed oligomers, are considered to be the most toxic species of the different assembly states that are the pathological components of neurodegenerative disorders. Therefore, a critical biomedical need exists for imaging probes that can identify and quantify them. We have designed and synthesized a novel fluorescent probe, **pTP-TFE** for which binding and selectivity profiles towards aggregated tau and Aβ proteins were assessed. Our results have shown **pTP-TFE** to be selective for early forms of soluble tau aggregates, with high affinity of dissociation constants (K_d) = 66 nM, and tenfold selectivity over mature tau fibrils. Furthermore, we found that **pTP-TFE** is selective for tau over Aβ aggregates and had good cell permeability. This selectivity of **pTP-TFE** towards early forms of aggregated tau protein *ex vivo* was also supported with studies on human brain tissue containing tau and Aβ pathology. To the best of our knowledge, this is the first fluorescent molecule to be reported to have this form of selectivity profile, which suggests that **pTP-TFE** is a unique probe candidate for imaging-based detection of early stages of Alzheimer's disease and other tauopathies.

Introduction

The accumulation of misfolded protein aggregates is a pathological hallmark of neurodegenerative diseases.[1] In the case of Alzheimer's disease (AD), the most prevalent pathology consists of extracellular β-amyloid protein (Aβ) plaques and intracellular tau protein-containing neurofibrillary tangles.[2] Protein aggregates have high beta-sheet structural characteristic,[3] which led to the identification of small molecules with specific binding affinity for them,[4] several of which have been used successfully for *in vivo* imaging with positron emission tomography (PET).[5] However, it is becoming increasingly apparent that proteins associated with neurodegenerative diseases can adopt different assembly states, which can impact disease onset and their progression to different extent.[6] Research on tau protein has shown that the earlier forming smaller soluble aggregates, generally termed oligomers, are the most toxic species and their *in vivo* levels are likely to be more correlated with disease progression than the levels of mature fibrils.[7] Given that early diagnosis of neurodegenerative disease has become an important objective, a critical need exists for the development of novel imaging probes that can identify and quantify soluble aggregated protein species *in vivo*. Moreover, such probes could greatly enhance our understanding of disease progression and be used for assessing the efficacy of new therapeutic candidates.

Efforts to design a facile imaging agent that can be used for investigation of soluble protein aggregates have thus far focused on Aβ-protein, leading to the development of a monoclonal antibody based probe ([^{125}I]8D3-F(ab′)2-h158)[8] and a modest number of small molecules, most notably BD-Oligo based on the boron-dipyrromethene (BODIPY) fluorescence structure[9] and AN-SP based on a spiropyran scaffold.[10] In addition, luminescent conjugated oligothiophenes (LCOs) have been shown to bind to soluble aggregates of both Aβ and tau protein.[11] Despite the success in recent years of developing PET probes for imaging tau neurofibrillary tangles[12] presently there are no probes that have selective binding toward tau soluble aggregated species. With tau protein pathology being a constituent feature of several neurodegenerative disorders, collectively termed tauopathies, the development of such probes, represents a major biomedical need.

[a]*Molecular Imaging Chemistry Laboratory, Wolfson Brain Imaging Centre, Department of Clinical Neurosciences, University of Cambridge, Cambridge, UK. E-mail: fia20@medschl.cam.ac.uk*

[b]*John van Geest Centre for Brain Repair, Department of Clinical Neuroscience, University of Cambridge, Cambridge, UK*

[c]*TTK-NAP B – Drug Discovery Research Group – Neurodegenerative Diseases, Institute of Organic Chemistry, Research Center for Natural Sciences, Budapest, Hungary*

[d]*Department of Chemistry, University of Cambridge, Lensfield Road, Cambridge, UK*

[e]*UK Dementia Research Institute, University of Cambridge, Cambridge, UK*

† Electronic supplementary information (ESI) available. See DOI: 10.1039/c9sc05620c

‡ These authors contributed equally.

The scaffold diversity of recently reported tau binding compounds highlights the fact that, despite recent progress, there is currently no clear structure activity relationship consensus. Nonetheless, flat π-conjugated scaffolds with length limited to 13 Å and polarizable ligands are thought to be essential design elements for tau probes.[13] Previously reported LCO, **pFTAA** (Scheme 1), fulfils these requirements by including a pentathiophene backbone and four carboxylic acid (CA) functional groups and has shown affinity for the soluble aggregates of tau and Aβ. However, with no apparent selectivity between protein types (*i.e.* tau or Aβ) or their various forms (*i.e.* soluble and fibril).[14–16]

Towards developing molecular imaging probes with selectivity for soluble aggregates we noted an important structural feature of mature tau fibrils is a positively charged flexible polyelectrolyte brush, also known as a fuzzy coat.[17] On the basis that the positive charges of the coat may interact strongly with the negative charges present in anionic dyes such as **pFTAA**, we reasoned that we may enhance selectivity toward soluble aggregate forms by reducing this chemical property.[18] To impart selectivity but retain the CA binding properties toward aggregated proteins, we chose to replace the CAs with bioisosteric 2,2,2-trifluoroethan-1-ol (TFE) functional groups, to yield the compound **pTP-TFE** (pentathiophene-trifluoroethanol – Scheme 1). TFE functional groups have been shown to act as excellent replacements for CA groups, while imparting superior pharmacokinetic properties on molecules.[19] Furthermore, the inclusion of fluorine into the molecule introduces several other advantages; (i) provides a natural position for labelling with fluorine-18 radioisotope so that a PET probe can be developed;[20] (ii) allows ^{19}F magnetic resonance imaging (MRI) and magnetic resonance spectroscopy (MRS) measurements; and (iii) may enhance *in vivo* pharmacokinetic properties, such as metabolic instability and reduce blood plasma retention.

Herein we report the synthesis of the novel fluorescent probe **pTP-TFE** as well as the characterization of its binding to tau and Aβ aggregated proteins in comparison to **pFTAA**. This includes the application of a sucrose gradient method to obtain known sizes of aggregate proteins and thereby quantify binding affinities of **pTP-TFE** towards specific soluble aggregated species. Finally, we assessed if **pTP-TFE** can penetrate intact live cell membranes and evaluated its binding to tau pathology in human brain tissue.

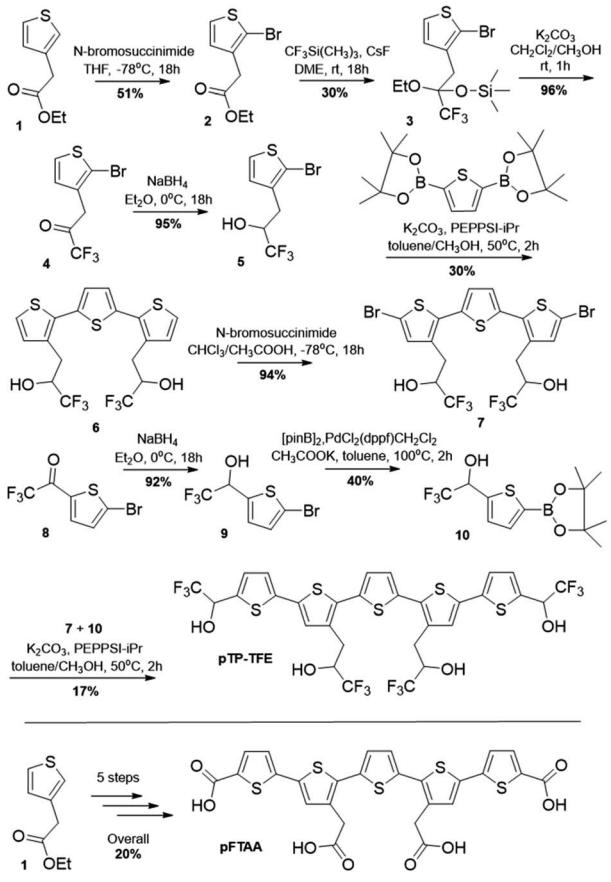

Scheme 1 Synthesis of pTP-TFE; synthesis of pFTAA (analogues to previously report).[14]

Results and discussion

Synthesis of pTP-TFE

The strategy for the synthesis of **pTP-TFE** relied on the trifluoromethylation of individual thiophene building blocks and their subsequent assembly to the pentameric target compound through Suzuki cross-coupling reactions (Scheme 1). Commercially available starting material (**1**) was brominated to yield **2** and subsequently treated with (trifluoromethyl)trimethylsilane and caesium fluoride to yield silyl protected compound **3**, which was purified, deprotected (**4**) and reduced to give 2,2,2-trifluoroethan-1-ol bearing thiophene **5**. **5** was cross-coupled to commercially available 2,5-bis-thiopheneboronic acid pinacol ester to yield **6**, which was brominated to give **7**. The terminal 2,2,2-trifluoroethan-1-ol bearing thiophene (**10**) was synthesized from commercially available starting material 2-bromo-5-trifluoroacetylthiophene (**8**), which was reduced (**9**) and subsequently boronated using bis(pinacolato)diboron (**10**). Finally, **pTP-TFE** was synthesized by Suzuki cross-coupling of substrates **7** and **10**. Purification of **pTP-TFE** by preparative thin-layer chromatography (TLC) afforded the compound in acceptable purity for *in vitro* evaluation. The overall yield for the synthesis of **pTP-TFE** from starting material (**1**) is 0.7%. **pFTAA** was synthesized from starting material (**1**), analogues to the previously reported methodology.[14] The fluorescence properties of **pTP-TFE** were obtained (Fig. S1.† **pTP-TFE**) including its quantum yield value, which at 0.27 is similar to **pFTAA**.[14]

Binding to Aβ and tau proteins in aggregation assay

We started our investigation into **pTP-TFE**'s binding and selectivity properties by performing an Aβ protein aggregation assay. In this assay monomeric Aβ40 is aggregated in the presence of **pTP-TFE** or **pFTAA** and the fluorescence intensities of the compounds monitored over time. An increase in fluorescence intensity is driven by realignment of π-orbitals due to conformation changes in the thiophene backbone and it is indicative of binding to protein aggregates.[14] Initial results were

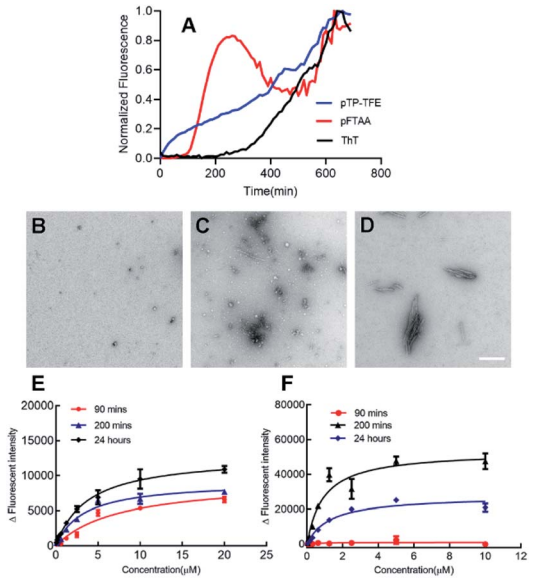

Fig. 1 (A) Normalized fluorescence intensities of **pTP-TFE**, **pFTAA** and **ThT** in an Aβ aggregation assay starting with Aβ40 monomers ($n = 3$). (B–D) Representative TEM image of Aβ aggregates 90 min (B), 200 min (C) and 700 min (D) (white bar = 200 nm). (E and F) Fluorescence intensity based binding curve of **pTP-TFE** (E) and **pFTAA** (F) with Aβ aggregates collected at 90 min (red), 200 min (blue) and 24 hours (black) of the aggregation assay.

encouraging as **pTP-TFE** showed an earlier response to Aβ40 aggregates in comparison to **pFTAA** (Fig. 1A). Transmission electron microscopy (TEM) images of Aβ40 aggregates at 90 min confirm the presence of small aggregate forms (Fig. 1B) and mature fibrils at later time points (700 min – Fig. 1D). To quantitatively assess the binding affinity of **pTP-TFE** and **pFTAA** to different types of aggregates, Aβ40 protein was collected from an aggregation assay (not containing compounds) at time points of 90 min, 200 min and 24 h. These aggregates were treated with different concentrations of the probes to determine binding constants (K_d) (Fig. 1E and F) by measuring their fluorescence intensity. These experiments confirmed that **pTP-TFE** displays a higher binding affinity to the earlier species (90 min) of aggregates ($K_d = 7.58$ μM), compared to **pFTAA** which showed no binding affinity for aggregates at this stage of maturation. Inversely, **pFTAA** showed stronger binding affinity to later aggregates ($K_d = 0.93$ μM {200 min}, $K_d = 0.65$ μM {24 h}) compared to **pTP-TFE** ($K_d = 3.27$ μM {200 min}, $K_d = 3.79$ μM {24 h}). In addition, the binding profile of **pTP-TFE** to a mixture of Aβ40 : Aβ42 (9 : 1 ratio), which is considered a more accurate representation of human cerebrospinal fluid Aβ aggregates *in vivo*, was also determined. On the basis of the analysis of fluorescence intensities during the assays (Fig. S6A†) **pTP-TFE** interacted with Aβ aggregates at an earlier time compared to **pFTAA** and **ThT**. Thus, we observe a similar relative interaction profile as with just Aβ40 (Fig. 1A). The binding affinities of **pTP-TFE** to Aβ40 : Aβ42 (9 : 1) mixture studied were $K_d = 2.1$ μM at 200 min and $K_d = 0.75$ μM at 24 h, therefore a higher binding affinity than just with Aβ40. This is consistent with higher affinity binding to Aβ42 as previously observed.[21]

We then investigated the binding profile of **pTP-TFE** to tau protein. To this end, tau monomers were subjected to fibril-forming conditions using heparin and aliquots removed at 1, 5, 24, 48, 80, 96, 168 and 240 h. Treatment of these aliquots with **pTP-TFE** showed a gradual increase of fluorescence intensity, which reached a maximum after 96 h and declined thereafter until the end point of the experiment (Fig. 2A). Experiments with **pFTAA** showed a curve of similar shape and characteristic trajectory.[16] TEM images of tau aggregates at different time points confirmed that initially small tau aggregates were detectable as early as 24 h (Fig. 2B), which became more apparent at 96 h (Fig. 2C) and then mature fibrils were found in the 240 h samples (Fig. 2D). These results suggest preferential binding of **pTP-TFE** to early soluble tau aggregates in comparison to **pFTAA**.

Interestingly, we observed a shift in the emission spectrum of **pTP-TFE** over the course of the experiment. Emission spectra recorded with tau aggregates at 24, 96 and 240 h show distinct shapes (Fig. S4A†). An analysis of the ratio of normalized fluorescence intensities at 495 nm and 560 nm revealed a gradual shift towards the blue until 96 h (ratio = 2.2 ± 0.20), followed by a shift back towards the red (ratio = 1.5 ± 0.74) (Fig. S4B†). These results suggest the **pTP-TFE** can bind to distinct oligomers of tau that are generated along the aggregation pathway of the protein. No emission spectrum shifts were observed in experiments with **pFTAA** (Fig. S5B†).

The binding affinity for **pTP-TFE** towards aggregates collected from the aggregation assay (not containing compounds) at 96 h and 240 h were determined by treatment with different concentrations of probe (Fig. 2E and F). **pTP-TFE** displayed exceptional affinity for small aggregates (96 h) with

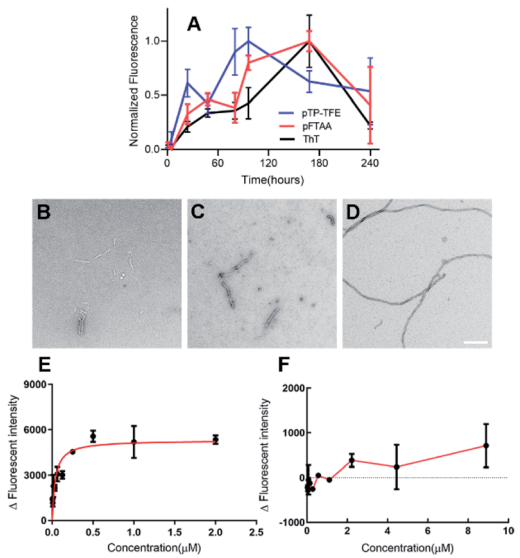

Fig. 2 (A) Normalized fluorescence intensities of **pTP-TFE** ($n = 3$), **pFTAA** ($n = 3$) and **ThT** ($n = 3$) in an aggregation assay starting with tau monomers. (B–D) Representative TEM image of tau aggregates 24 h (B), 96 h (C) and 240 h (D) (white bar = 200 nm). (E and F) Binding affinity of **pTP-TFE** to tau aggregates collected at 96 hours (E) and 240 hours (F) of the aggregation assay.

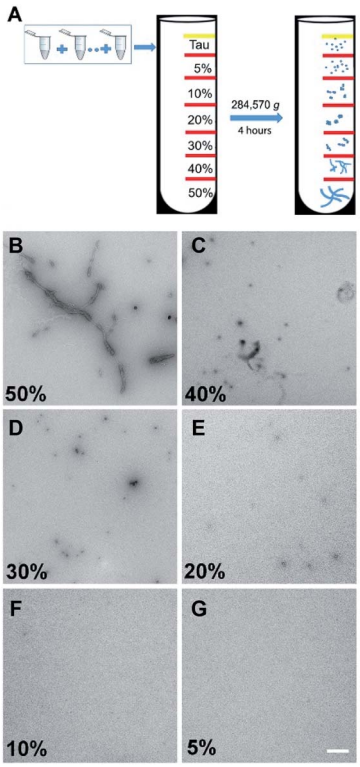

Fig. 3 (A) Tau (0N4R) protein were collected in 100 μL aliquots every 24 hours from the aggregation reaction and then stored at −80 °C after flash freezing. After 240 hours of incubation 1 mL of tau aggregates was collected and loaded on the top of the ultracentrifuge. (B–G) TEM images of tau aggregates structures at fractions from 50% to 5% sucrose gradient after 4 hours of ultracentrifugation (white bar = 500 nm).

a K_d of 38 nM and, encouragingly, showed no detectable affinity towards the 240 h tau fibril sample (K_d < 10 μM). These results indicate good selectivity towards soluble aggregated species.

Binding to fractionated aggregates of Aβ and tau proteins

It has been well documented that protein samples collected at different time points of an aggregation assay contain heterogeneous mixtures of different aggregated species, from small soluble forms to fibrils. Therefore, we recognized the need to purify these samples to obtain homogenous protein aggregate fractions of tau in order to confirm the binding profile discussed above. To achieve this, we employed a sucrose gradient ultracentrifugation technique by means of which protein aggregates of different sizes can be separated into homogenous fractions[22] and then used these samples for affinity measurement (Fig. 3).

The binding affinities of **pTP-TFE** and **pFTAA** with 10% to 50% sucrose gradient tau aggregates were then tested by a fluorescent binding assay (Table 1). The data obtained confirms results from the previous experiments (Fig. S7†) indicating **pTP-TFE** binds most strongly to the 20% sucrose gradient fraction (K_d = 66 nM), which consist of soluble aggregated tau as confirmed by TEM (Fig. 3). Furthermore, selectivity of **pTP-TFE** for small aggregates over fibrils was confirmed by a difference in K_d for 40% and 50% sucrose gradient tau aggregates of approximately one order of magnitude. Comparisons of **pTP-TFE** to tau binding affinity data with that to Aβ aggregates at 200 min (Table 1) show a 50-fold selectivity in favour of tau (K_d(Aβ40) = 3.3 μM *vs.* K_d(tau) = 66 nM). This indicates that **pTP-TFE** is also selective for soluble tau aggregates over soluble Aβ aggregates. **pFTAA**, by comparison, displays highest affinity to tau aggregates in the 50% sucrose gradient fraction (K_d = 0.20 μM) and Aβ fibril aggregates (24 h; K_d = 0.65 μM; Table 1). These results support our hypothesis that the removal of negatively charged functional groups imparts higher selectivity for early aggregates of tau over mature fibrils. Encouragingly, these results also show that the use of TFE bioisostere endows the compound with selectivity for soluble aggregates of tau over soluble aggregates of Aβ.

Cellular uptake of pTP-TFE into primary human fetal neurons

To determine whether **pTP-TFE** can penetrate live intact cell membranes we investigated the cellular uptake of **pTP-TFE** in live primary human fetal neurons. This was performed by adding **pTP-TFE** to a final concentration of 4 μM in a culture medium, and incubating for 15 min, 30 min, 60 min and 120 min. **pTP-TFE** uptake in neurons at each time point was determined by acetonitrile extraction of PBS-washed cultures, and quantified using an LC-MS/MS assay[23] (Fig. S9†). This

Table 1 Binding affinity of pTP-TFE and pFTAA with 10% to 50% tau fraction (n = 3–6) and Aβ40 aggregates at 90 min, 200 min and 24 hours (n = 3) after ultracentrifugation, K_d values were fitted using GraphPad Prism5

Aggregates	**pTP-TFE**, K_d (μM)	**pTP-TFE**, binding ratio[a]	**pFTAA**, K_d (μM)	**pFTAA**, binding ratio[b]
10% Sucrose tau	0.96 ± 0.20	14	29.57 ± 2.10	148
20% Sucrose tau	0.07 ± 0.03	1	2.75 ± 0.57	14
30% Sucrose tau	3.04 ± 0.71	49	5.27 ± 1.25	26
40% Sucrose tau	0.59 ± 0.20	9	1.29 ± 0.20	6
50% Sucrose tau	1.08 ± 0.17	15	0.20 ± 0.01	1
90 Minute, Aβ	7.58 ± 2.47	108	No affinity	N/A
200 Minute, Aβ	3.27 ± 0.64	47	0.93 ± 0.30	5
24 Hour, Aβ	3.79 ± 0.34	54	0.65 ± 0.19	3

[a] Binding ratio is based on comparison of K_d values with the 20% sucrose tau K_d. [b] Binding ratio is based on comparison of K_d values with the 50% sucrose tau K_d.

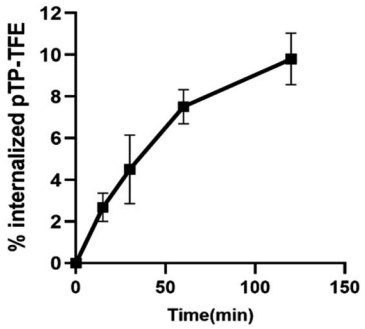

Fig. 4 Kinetics of **pTP-TFE** uptake in primary human fetal neurons quantified by measuring the concentration of **pTP-TFE** in live neurons using LC-MS/MS; data presented as % of total administered amount. *Y* values calculated from Table S1† ($n = 3$).

showed 5% of the total applied **pTP-TFE** in the neuronal cells within 30 min and 10% in 2 hours (Fig. 4 and Table S1†), which indicates the compound can cross the cell membrane with rapid uptake. The quantity and kinetics of this uptake are comparable to other compounds, including established PET probes in oncology[24] and agents delivered into neuronal cells.[25]

Ex vivo imaging of early tau aggregates in AD and PSP human brain slices

Finally, we investigated whether the selectivity demonstrated in *in vitro* assays could be replicated in *ex vivo* human brain tissue. To this end we evaluated the binding of **pTP-TFE** to tau pathology in human brain tissue of progressive supranuclear palsy (PSP), a pure tauopathy, and Alzheimer's disease, which contains both Aβ and tau pathology. Low-magnification epifluorescence microscopy showed that **pTP-TFE** signals can be found colocalizing with hyperphosphorylated, AT8-positive tau pathology in both PSP and AD brains (Fig. 5A). Closer inspection using confocal microscopy revealed that **pTP-TFE** signals were predominantly observed within the cell soma, co-localizing with AT8-positive tau pathology, although the presence of **pTP-TFE** signals could also be found in the axonal/dendritic compartments (Fig. 5B, arrows). Conversely, co-localization with tau fibril antibody AT100 is less well established; AT100-positive immunoreactivity has been shown to selectively label filamentous tau pathology,[26] this substantiates our *in vitro* binding data and suggests that **pTP-TFE** demonstrates preferential reactivity to early stage soluble tau aggregates.

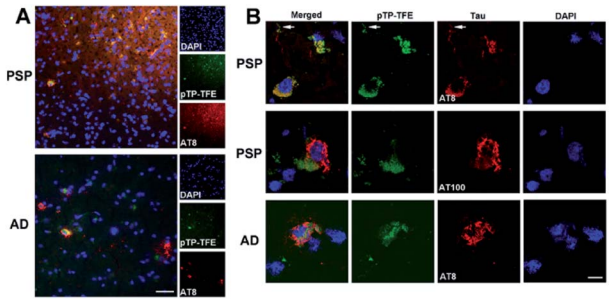

Fig. 5 **pTP-TFE** staining with human PSP ($n = 5$) and AD brain slides ($n = 4$). (A) Epifluorescence images of **pTP-TFE** in AD and PSP human brain slides with scale bar = 50 μm. (B) Confocal images of **pTP-TFE** in AD and PSP with scale bar = 10 μm. The arrows indicate an axonal/dendritic compartment.

Conclusions

We have designed and synthesized a novel fluorescent probe, **pTP-TFE** for which binding and selectivity profiles towards aggregated tau and Aβ proteins were assessed. This included use of a sucrose gradient ultracentrifugation method for more accurate quantification of binding affinities to specific size tau aggregates. Our results show **pTP-TFE** to be selective for soluble tau aggregates, with a high affinity of $K_d = 66$ nM, and ten-fold selectivity over mature fibrils. Furthermore, we found that **pTP-TFE** is tau selective over Aβ, the other major misfolded protein aggregate of neurodegenerative disorders. To the best of our knowledge, **pTP-TFE** is the first fluorescent molecule to have this form of selectivity for soluble tau aggregates over tau fibrils. In addition, we established that **pTP-TFE** could penetrate intact live cell membranes rapidly, while its selectivity towards early forms of aggregated tau protein was also supported by studies on human brain tissue containing tau and Aβ pathology.

The high affinity and selectivity for early soluble aggregates of tau and its cell permeability make **pTP-TFE** a best in class molecular tool for the study of tauopathy development and progression as well as a proof of concept chemotype for the development of small molecule therapeutics, with enhanced affinity and selectivity. We aim to utilize the potential displayed by **pTP-TFE** *in vitro* and *ex vivo* through *in vivo* optical, fluorine-19 MRI/MRS and fluorine-18 PET imaging modalities in the future.

Conflicts of interest

There are no conflicts to declare.

Acknowledgements

The authors thank Dr Gabriele Schierle and Dr Na Yu (Chemical Engineering Department, University of Cambridge), Dr Karin Muller (Cambridge Advanced Imaging Center) for technical support, Prof James Rowe (Department of Clinical Neurosciences, University of Cambridge), Dr David Williamson and Cambridge Brain Bank for the post-mortem brain samples, EPSRC Mass Spectrometry Service (University of Swansea). Cambridge Brain Bank is supported by the NIHR Cambridge Biomedical Research Centre. This study was funded by the National Institute for Health Research (NIHR) Cambridge Biomedical Research Centre: Dementia and Neurodegeneration theme, Medical Research Council grant (MR/K02308X/1), the Engineering and Physical Sciences Research Council (ST, EP/P008224/1), Royal Society (DK), and Amgen Foundation Scholarship (ER). WLK and BV are supported by the Medical Research

Council (MR/S005528/1). GT was supported by the Hungarian Brain Research Program (2017-1.2.1-NKP-2017-00002).

Notes and references

1 F. Chiti and C. M. Dobson, *Annu. Rev. Biochem.*, 2006, **7**, 333.
2 C. Ballatore, V. M. Lee and J. Q. Trojanowski, *Nat. Rev. Neurosci.*, 2007, **8**, 663; L. M. Ittner and J. Götz, *Nat. Rev. Neurosci.*, 2011, **12**, 67; B. Ghetti, A. L. Oblak, B. F. Boeve, K. A. Johnson, B. C. Dickerson and M. Goedert, *Neuropathol. Appl. Neurobiol.*, 2015, **41**, 24.
3 E. D. Eanes and G. G. Glenner, *J. Histochem. Cytochem.*, 1968, **16**, 673; A. W. Fitzpatrick, B. Falcon, S. He, A. G. Murzin, G. Murshudov, H. J. Garringer, R. A. Crowther, B. Ghetti, M. Goedert and S. H. Scheres, *Nature*, 2017, **547**, 185.
4 M. R. Jones, E. Mathieu, C. Dyrager, S. Faissner, Z. Vaillancourt, K. J. Korshavn, M. H. Lim, A. Ramamoorthy, V. W. Yong, S. Tsutsui and P. K. Stys, *Chem. Sci.*, 2017, **8**, 5636; Y. Li, D. Xu, A. Sun, S. L. Ho, C. Y. Poon, H. N. Chan, O. T. Ng, K. K. Yung, H. Yan, H. W. Li and M. S. Wong, *Chem. Sci.*, 2017, **8**, 8279; K. P. Nilsson, *FEBS Lett.*, 2009, **583**, 2593.
5 Y. Liu, Y. Yang, M. Sun, M. Cui, Y. Fu, Y. Lin, Z. Li and L. Nie, *Chem. Sci.*, 2017, **8**, 2710; A. Nordberg, J. O. Rinne, A. Kadir and B. Långström, *Nat. Rev. Neurol.*, 2010, **6**, 78.
6 D. Eisenberg and M. Jucker, *Cell*, 2012, **148**, 1188; J. L. Guo, D. J. Covell, J. P. Daniels, M. Iba, A. Stieber, B. Zhang, D. M. Riddle, L. K. Kwong, Y. Xu, J. Q. Trojanowski and V. M. Lee, *Cell*, 2013, **154**, 103.
7 S. Maeda, N. Sahara, Y. Saito, S. Murayama, A. Ikai and A. Takashima, *Neurosci. Res.*, 2006, **54**, 197; M. Goedert, *Alzheimers Disease & Dementia*, 2016, **12**, 1040.
8 D. Sehlin, X. T. Fang, L. Cato, G. Antoni, L. Lannfelt and S. Syvänen, *Nat. Commun.*, 2016, **7**, 10759.
9 C. L. Teoh, D. Su, S. Sahu, S. W. Yun, E. Drummond, F. Prelli, S. Lim, S. Cho, S. Ham, T. Wisniewski and Y. T. Chang, *J. Am. Chem. Soc.*, 2015, **137**, 13503; L. P. Jameson and S. V. Dzyuba, *Bioorg. Med. Chem. Lett.*, 2013, **23**, 1732; S. Lim, M. M. Haque, D. Su, D. Kim, J. S. Lee, Y. T. Chang and Y. K. Kim, *Chem. Commun.*, 2017, **53**, 1607.
10 G. Lv, A. Sun, P. Wei, N. Zhang, H. Lan and T. Yi, *Chem. Commun.*, 2016, **52**, 8865.
11 T. Klingstedt, H. Shirani, K. A. Åslund, N. J. Cairns, C. J. Sigurdson, M. Goedert and K. P. Nilsson, *Chem.–Eur. J.*, 2015, **19**, 10179.
12 V. L. Villemagne, V. Doré, S. C. Burnham, C. L. Masters and C. C. Rowe, *Nat. Rev. Neurol.*, 2018, **14**, 225; M. Goedert, Y. Yamaguchi, S. K. Mishra, M. Higuchi and N. Sahara, *Frontiers in Neurology*, 2018, **15**, 70.
13 P. Verwilst, H. S. Kim, S. Kim, C. Kang and J. S. Kim, *Chem. Soc. Rev.*, 2018, **47**, 2249.
14 A. Åslund, C. J. Sigurdson, T. Klingstedt, S. Grathwohl, T. Bolmont, D. L. Dickstein, E. Glimsdal, S. Prokop, M. Lindgren, P. Konradsson and D. M. Holtzman, *ACS Chem. Biol.*, 2009, **4**, 673.
15 T. Klingstedt and K. P. Nilsson, *Biochem. Soc. Trans.*, 2012, **40**, 704.
16 T. Klingstedt, H. Shirani, J. Mahler, B. M. Wegenast-Braun, S. Nyström, M. Goedert, M. Jucker and K. P. Nilsson, *Chem.–Eur. J.*, 2015, **21**, 9072.
17 J. E. Gerson and R. Kayed, *Frontiers in Neurology*, 2013, **17**, 93; L. D. León, I. Karla, P. García-Gutiérrez, I. N. Serratos, M. Palomera-Cárdenas, M. D. Figueroa-Corona, V. Campos-Peña and M. A. Meraz-Ríos, *J. Alzheimer's Dis.*, 2013, **35**, 319.
18 C. A. Lasagna-Reeves, D. L. Castillo-Carranza, U. Sengupta, M. J. Guerrero-Munoz, T. Kiritoshi, V. Neugebauer, G. R. Jackson and R. Kayed, *Sci. Rep.*, 2012, **2**, 700.
19 C. Ballatore, D. M. Huryn and A. B. Smith, *ChemMedChem*, 2013, **8**, 385; Y. Ducharme, M. Blouin, M. C. Carrière, A. Chateauneuf, B. Côté, D. Denis, R. Frenette, G. Greig, S. Kargman, S. Lamontagne and E. Martins, *Bioorg. Med. Chem. Lett.*, 2005, **15**, 1155.
20 P. Nordeman, L. B. Johansson, M. Bäck, S. Estrada, H. Hall, D. Sjölander, G. T. Westermark, P. Westermark, L. Nilsson, P. Hammarström and K. P. Nilsson, *ACS Med. Chem. Lett.*, 2016, **7**, 368.
21 G. Yamin and D. B. Teplow, *J. Neurochem.*, 2017, **140**, 210; A. Jan, O. Gokce, R. Luthi-Carter and H. A. Lashuel, *J. Biol. Chem.*, 2008, **283**, 28176.
22 S. Maeda, N. Sahara, Y. Saito, M. Murayama, Y. Yoshiike, H. Kim, T. Miyasaka, S. Murayama, A. Ikai and A. Takashima, *Biochemistry*, 2007, **46**, 3856.
23 J. Bhat, A. Narayan, J. Venkatraman and M. Chatterji, *J. Microbiol. Methods*, 2013, **94**, 152; K. H. Richards, N. Schanze, R. Monk, E. Rijntjes, D. Rathmann and J. A. Köhrle, *PLoS One*, 2017, **12**, 1.
24 M. G. MacAskill, A. S. Tavares, J. Wu, C. Lucatelli, J. C. Mountford, A. H. Baker, D. E. Newby and P. W. Hadoke, *Sci. Rep.*, 2017, **7**, 44233.
25 L. Hasadsri, J. Kreuter, H. Hattori, T. Iwasaki and J. M. George, *J. Biol. Chem.*, 2009, **284**, 6972.
26 F. Clavaguera, H. Akatsu, G. Fraser, R. A. Crowther, S. Frank, J. Hench, A. Probst, D. T. Winkler, J. Reichwald, M. Staufenbiel, B. Ghetti, M. Goedert and M. Tolnay, *Proc. Natl. Acad. Sci. U. S. A.*, 2013, **110**, 9535.

